Quantum-state measurement of two-mode entangled field-state in a high-Q cavity

Ashfaq H. Khosa[1] and M. Suhail Zubairy[2]
[1]*Department of Electronics, Quaid-i-Azam University, Islamabad, Pakistan*
[2]*Institute for Quantum Studies, and Department of Physics, Texas A&M University, College Station, Texas 77843-4242, USA*
(Received 3 July 2005; published 17 October 2005)

We propose a scheme for the measurement of a two-mode entangled field-state in a high-Q cavity. The scheme utilizes the momentum distribution spectrum in the Raman-Nath regime of a three-level atom in V configuration. Due to the two modes of the electromagnetic field the atom may have x interactions with mode A, and y interactions with mode B, causing a complex momentum distribution. The momentum distribution of the atom after interaction with the quantized cavity fields contains the information of the field photon statistics. We reconstruct the joint photon statistics of the entangled field with the help of recorded momentum spectrum. We also propose to reconstruct the Wigner function of a two-mode entangled field state by injecting two coherent states resonant to each mode into the cavity and then measuring the joint photon statistics of the displaced field.

DOI: 10.1103/PhysRevA.72.042106 PACS number(s): 03.65.Ta, 42.50.Ar, 03.75.Be, 03.65.Ud

I. INTRODUCTION

The quantum theory of physics has been a fascinating playground to study the nature of electromagnetic radiations. The recent interests in this subject arose not only because of the interests in basic atom-field interaction but also the stream of study is due to the fascination in the measurement of the quantum state of an unknown field-state in high-Q cavities. The great interest in the measurement of the cavity field is due to its application in the newly progressing field of quantum informatics [1–4]. For the measurement of the quantum state one needs to do a set of experiments on the identically prepared quantum systems. The reason to do so is the fundamental constraint of the quantum physics which states that a single experiment on a quantum system reveals only limited aspects of the system.

Smithy and co-workers [5] have given the first experimental report on the reconstruction of the quantum state of a radiation field. They used optical tomography proposed by Vogel and Risken [6] for the reconstruction of quantum state of a single mode radiation field. The Wigner function of the field mode has been obtained (from the distribution measured in balance homodyne) using Radon transformation [6].

Besides the homodyne detection method several other possibilities have also been explored for the reconstruction of the quantum state of an electromagnetic field. These schemes are based on the Ramsey method of separated oscillatory fields [7], absorption and emission spectra [8], and the atomic beam deflection [9–14]. The atomic deflection method, which uses the momentum distribution of the atoms in order to reveal the quantum state of light inside the cavity, provides a nice tool for this purpose. It is well-known that the momentum distribution of the deflected atoms is a function of field photon numbers [10,12–14]. The atomic diffraction from the electromagnetic field may be divided into two regimes, one in which the recoil energy of the field is much less then the Rabi frequency (Raman-Nath regime [10,13]) and the other in which the recoil energy is much greater than the Rabi frequency (the Bragg's regime [12,14–16]). Here we are concerned with the atomic beam diffraction with the cavity field in the Raman-Nath regime, which is used for the reconstruction of two entangled modes of the cavity field.

Several types of entangled field states [17] have been discussed in literature and also there are many schemes for the measurement of the quantum statistical properties of the entangled field modes [18–24]. Among them the scheme of Kim and Agarwal [19] uses the probability of atomic inversion and relates it to the Wigner characteristic function [20]. Ikram and Zubairy use Autler-Townes spectroscopy to reconstruct the two-mode entangled state in a high-Q cavity [22], and Davidovich *et al.* use the Ramsey type setup to reconstruct the GHZ state [23]. Having a well justified and mathematically tractable measure of entangled field-state is likely to be of high value in new developing fields of quantum computing [1], quantum teleportation [2], dense coding [3], and quantum cryptography [4]. The feasibility of some of these applications has been demonstrated in recent experiments.

The model we propose here concerns the measurement of the joint photon statistics and the Wigner function of the *bi*-mode quantized entangled electromagnetic fields in a single high-Q cavity. The scheme utilizes the Raman-Nath diffraction of the three-level atoms from the standing wave field. Previously we have suggested a scheme for the reconstruction of the single mode cavity field [13]. Now, we extend the idea to a two-mode entangled field-state. The proposal suggests to put a slit with width much smaller than the wavelengths of the two modes in front of the cavity as was used by Herkommer *et al.* [10]. The atoms are injected through the slit so that they may interact with a small portion of the standing wave field. After the interaction we measure the momentum distribution of the atoms behind the cavity. The momentum distribution of the atomic beam shows a complex behavior as compared to the single mode field in a high-Q cavity [13]. This uneven distribution is due to the simultaneous interaction of n photons of mode A and m photons of mode B with a three-level atom. We utilize this spectrum which yields a successful reconstruction of the joint photon statistics of the two-mode entangled electromagnetic field.

The joint photon statistics of the two-mode entangled field-state gives only the diagonal elements of the density matrix. For the off-diagonal density matrix elements we propose to reconstruct the Wigner function of the entangled field-state. For this we propose to displace the photon statistics of each mode of the field by injecting the resonant coherent states [25] into the cavity. This displaced photon statistics may be used to reconstruct the Wigner function $W(\alpha, \alpha^*, \beta, \beta^*)$ of the entangled state of the cavity modes in a straightforward manner [22,26].

II. THE CONDITIONS FOR RAMAN-NATH AND BRAGG'S DIFFRACTION

In the Raman-Nath regime the atom after the interaction with the field may have many possible diffraction orders simultaneously [10,13], while in Bragg's regime the atom has only two possible output states [12,14,16] (i.e., it may go undeflected or get deflected with the same order). The reason for many possible diffraction orders in the Raman-Nath diffraction process is that the atomic de Broglie wave is very sharply focused (which is contrary to Bragg's scattering). The absorption and stimulated emission of photon pairs causes the change in the direction of momentum of the atom along the wave propagation direction.

The condition for the Raman-Nath regime is that the recoil energy must be much less than the energy associated with the Rabi frequency and it is achieved in the limit

$$\frac{\hbar k^2}{2M} \ll \frac{g\sqrt{m}}{2}, \tag{1}$$

while the condition for the Bragg's regime is contrary to the Raman-Nath regime, i.e.,

$$\frac{\hbar k^2}{2M} \gg \frac{g\sqrt{m}}{2}, \tag{2}$$

where M is the mass of the atom, g is the coupling constant, and m is the number of photons in the cavity.

III. MODEL FOR THE RECONSTRUCTION

We consider the case of a high-Q cavity containing two entangled modes of standing wave electromagnetic field. In this section, we propose a scheme for the measurement of the joint photon statistics, i.e., $p(n,m)$, of the entangled modes of the cavity field, where n and m represent the number of photons in mode A and B, respectively.

A three-level atom in V configuration interacts with the standing wave field of the two entangled modes as shown in Fig. 1. The upper two levels of the atoms are labeled as $|a\rangle$ and $|c\rangle$ and the lower level is denoted by $|b\rangle$. We choose the atoms that have $|b\rangle \leftrightarrow |a\rangle$ transition resonant with mode A and $|b\rangle \leftrightarrow |c\rangle$ transition resonant with mode B of the cavity field, while $|a\rangle \leftrightarrow |c\rangle$ transition is forbidden. The Hamiltonian of the atom-field system in interaction picture under dipole and rotating-wave approximation is

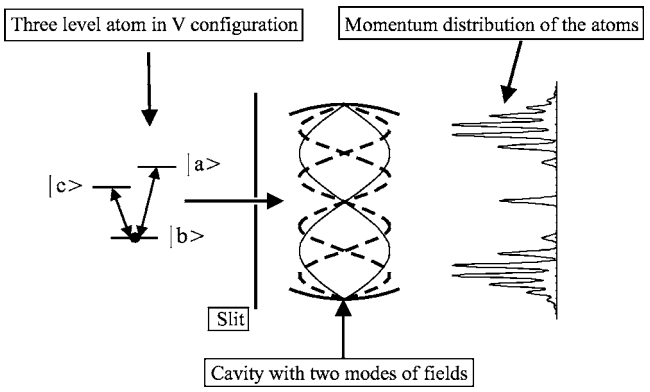

FIG. 1. Schematics of a three-level atom in V configuration interacting with a bi-mode standing wave entangled field in high-Q cavity. After the interaction with the standing wave fields, the diffracted atoms show a momentum distribution spectrum. A slit of width $\delta x \ll \lambda_i$ allows the atoms to interact with a small portion of the standing wave electromagnetic field. The Wigner function can be reconstructed for the cavity entangled modes by injecting the same mode coherent state for different phases.

$$H = \frac{\hat{P}^2}{2M} + \hbar g_A \sin(k_A \hat{x})(\sigma_{A+} a + \sigma_{A-} a^\dagger) + \hbar g_B \sin(k_B \hat{x})(\sigma_{B+} b + \sigma_{B-} b^\dagger), \tag{3}$$

where $\sigma_{A+}=|a\rangle\langle b|$, $\sigma_{A-}=|b\rangle\langle a|$, $\sigma_{B+}=|c\rangle\langle b|$, and $\sigma_{B-}=|b\rangle\langle c|$ are the usual atomic raising and lowering operators, and $a(a^\dagger)$ and $b(b^\dagger)$ are the creation (annihilation) operators of the mode A and B, respectively. Similarly g_A and g_B are the coupling constants of the atom-field interaction with mode A and B, respectively. $\hat{P}^2/2M$ is the kinetic energy which contains the momentum contribution in the Hamiltonian.

On their way to the cavity, the atoms pass through a slit which we place in front of the standing modes of the field. We propose to use the slit of width much less than the wavelengths of the standing wave cavity modes, i.e., $\delta x \ll \lambda_A$ and $\delta x \ll \lambda_B$, where δx is the width of the slit, and λ_A and λ_B are the wavelengths of mode A and B, respectively [10]. This situation leads to the approximation in which one can replace the usual $\sin(k_i \hat{x})$ dependence with $k_i \hat{x}$, where $k_i = k_A, k_B$ (wave vectors of the cavity modes A and B, respectively). Furthermore, we consider the Raman-Nath regime, where it is assumed that the momentum component of the atoms along the transverse direction is very large so it can be treated classically and the contribution of the momentum term in the Hamiltonian can be neglected [10,13]. Here we neglect the incoherent processes such as the damping of the cavity and the spontaneous emission from the atoms, which are achievable with the current technology under the appropriate selection of the parameters.

We deal with the problem in density matrix approach governed by

$$\dot{\rho} = \frac{-i}{\hbar}[H, \rho]. \tag{4}$$

We find the equations of motion for the density matrix elements in the case of proposed three-level atom interacting

with two quantized cavity modes. This set of coupled differential equations is solved using Laplace transform. We make use of the initial condition that the atoms are prepared in ground state $|b\rangle$ before interaction with the cavity modes. The solution to the set of equations is given in the Appendix. Here we write only the density matrix elements of the three atomic states that we want to exploit for the measurement of the joint photon statistics of the cavity field, i.e.,

$$\rho^{b,b}_{nm,nm}(x,x',t) = \frac{1}{2}\{\cos[(x-x')\eta t] + \cos[(x+x')\eta t]\}\rho^{b,b}_{nm,nm}(x,x',0), \quad (5)$$

$$\rho^{a,a}_{n-1m,n-1m}(x,x',t) = \frac{\alpha^2}{2\eta^2}\{\cos[(x-x')\eta t] - \cos[(x+x')\eta t]\}\rho^{b,b}_{nm,nm}(x,x',0), \quad (6)$$

$$\rho^{c,c}_{nm-1,nm-1}(x,x',t) = \frac{\beta^2}{2\eta^2}\{\cos[(x-x')\eta t] - \cos[(x+x')\eta t]\}\rho^{b,b}_{nm,nm}(x,x',0), \quad (7)$$

where in the above set of equations

$$\eta = \sqrt{\alpha^2+\beta^2}, \quad (8)$$

along with $\alpha = g_A k_A \sqrt{n}$ and $\beta = g_B k_B \sqrt{m}$. We realize that the η [expressed in Eq. (8) and a function of the two wave vectors k_A and k_B along with the two vacuum Rabi frequencies associated with the cavity mode A and B] can be expressed as a function of a one wave vector and one coupling constant. We obtain this by defining $k_A = \varepsilon k_B$, and $g_A = \xi g_B$, where ε and ξ are dimensionless constants. This substitution in Eq. (8) leads to

$$\eta = k_B g_B \eta', \quad (9)$$

where the new function η' depends only on the set of joint photon numbers, i.e.,

$$\eta' = \sqrt{\xi^2\varepsilon^2 n + m}. \quad (10)$$

The expression of η in the form of Eq. (9) makes the calculations very simple for further proceedings.

The density operator in the momentum representation is defined as

$$\rho(\wp,t) = \frac{1}{2\pi\hbar}\int_{-\infty}^{\infty}\frac{d\theta}{k}\int_{-\infty}^{\infty}\frac{d\theta'}{k}\rho(\theta',\theta,t)\exp[i\wp(\theta'-\theta)], \quad (11)$$

where $\wp = p/\hbar k$ and $\theta = kx$ denote the normalized momentum and position, respectively. The resulting expressions for the density matrix elements [Eqs. (5)–(7)] in momentum space are given by

$$\rho^{b,b}_{nm,nm}(\wp,t) = \left(\frac{1}{2\pi\hbar}\right)\left(\frac{1}{4}\right) \times \int_{-\infty}^{\infty}\frac{d\theta_B}{k_B}(e^{-i(\wp-\acute{\eta}\kappa)\theta_B} + e^{-i(\wp+\acute{\eta}\kappa)\theta_B}) \times \int_{-\infty}^{\infty}\frac{d\theta'_B}{k_B}(e^{i(\wp-\acute{\eta}\kappa)\theta'_B} + e^{i(\wp+\acute{\eta}\kappa)\theta'_B}) \times \rho^{b,b}_{nm,nm}(\theta_B,\theta'_B,0), \quad (12)$$

$$\rho^{a,a}_{n-1m,n-1m}(\wp,t) = \left(\frac{1}{2\pi\hbar}\right)\left(\frac{\xi^2\varepsilon^2 n}{4\acute{\eta}^2}\right) \times \int_{-\infty}^{\infty}\frac{d\theta_B}{k_B}(e^{-i(\wp-\acute{\eta}\kappa)\theta_B} - e^{-i(\wp+\acute{\eta}\kappa)\theta_B}) \times \int_{-\infty}^{\infty}\frac{d\theta'_B}{k_B}(e^{i(\wp-\acute{\eta}\kappa)\theta'_B} - e^{i(\wp+\acute{\eta}\kappa)\theta'_B}) \times \rho^{b,b}_{nm,nm}(\theta_B,\theta'_B,0), \quad (13)$$

$$\rho^{c,c}_{nm-1,nm-1}(\wp,t) = \left(\frac{1}{2\pi\hbar}\right)\left(\frac{m}{4\acute{\eta}^2}\right) \times \int_{-\infty}^{\infty}\frac{d\theta_B}{k_B}(e^{-i(\wp-\acute{\eta}\kappa)\theta_B} - e^{-i(\wp+\acute{\eta}\kappa)\theta_B}) \times \int_{-\infty}^{\infty}\frac{d\theta'_B}{k_B}(e^{i(\wp-\acute{\eta}\kappa)\theta'_B} - e^{i(\wp+\acute{\eta}\kappa)\theta'_B}) \times \rho^{b,b}_{nm,nm}(\theta_B,\theta'_B,0), \quad (14)$$

where $\kappa = g_B t$. We find the momentum distribution of the atoms at the detection system by taking the trace over the internal atomic states and the field-states. Thus the probability of the atom with momentum $\wp$ is given by

$$W(\wp) = \sum_{n,m}[\rho^{a,a}_{n-1m,n-1m}(\wp,t) + \rho^{b,b}_{nm,nm}(\wp,t) + \rho^{c,c}_{nm-1,nm-1}(\wp,t)]. \quad (15)$$

Now let $g(\theta_B/k_B)$ be the distribution function of the atoms at the slit. The modulus square of $g(\theta_B/k_B)$ gives the probability of finding the atoms at position x. We consider $p(n,m)$ to be the joint probability of the n photons in the cavity mode A and m photons in the cavity mode B. Also we consider the situation where the atoms and the cavity field are unentangled at $t=0$. This situation is expressed as follows:

$$\rho^{b,b}_{nm,nm}(\theta'_B,\theta_B,0) = \sum_{n,m} g(\theta'_B/k_B)(g\,\theta_B/k_B)p(n,m). \quad (16)$$

A substitution of the density matrix elements [i.e., Eqs. (12)–(14)] along with the initial condition defined in Eq. (16) for the probability of atoms with momentum $\wp$ [i.e., Eq. (15)] gives

$$W(\wp) = \sum_{n,m} [\{|f_{(+)}|^2 + |f_{(-)}|^2\} p(n,m)], \tag{17}$$

where

$$f_{(\pm)} = \frac{1}{2\sqrt{\pi\hbar}} \int_{-\infty}^{\infty} \frac{d\theta_B}{k_B} e^{-i(\wp/\kappa \pm \eta')\theta_B} g(\theta_B/k_B) \tag{18}$$

is the momentum distribution function. Let us consider a normalized Gaussian distribution for the atoms at the slit, i.e.,

$$g(\theta_B/k_B) = \left(\frac{1}{\pi \delta x^2}\right)^{1/4} \exp[-\theta_B^2/2\delta x^2 k_B^2], \tag{19}$$

we arrive at the following expression of the momentum distribution function:

$$f_{(\pm)} = \left(\frac{\delta x^2}{4\pi\hbar^2}\right)^{1/4} \exp[-(\wp/\kappa \pm \eta')^2 \kappa^2 \delta x^2 k_B^2/2]. \tag{20}$$

The expression (20) indicates that we get the peaks whenever η', which is basically a set of joint photon numbers, equates to the normalized momentum $\wp$ divided by κ. This expression makes the fact evident that the momentum distribution is dependent on the set of joint photon numbers present in the cavity. Hence one can reconstruct the joint photon statistics of the cavity field-state from the recorded momentum distribution. From Eq. (20) it is also clear that the separation between the peaks of the momentum spectrum depends on the parameters of the atom-field interaction, especially κ, which contains the vacuum Rabi frequency g_B. The graphs indicate that $f_{(+)}$ selects the negative side of the momentum axis and $f_{(-)}$ results to the positive side. Both of them have identical peaks. For $\wp/\kappa = 0$ the peak height is double due to the contribution of both terms, i.e., $f_{(+)}$ and $f_{(-)}$. One can use either the positive or negative side of the momentum distribution spectrum for the reconstruction of the joint photon statistics of the cavity field.

The selection of the product of constants in $\acute{\eta}$ is tricky. For finding these constants, we plot the momentum distribution of the atoms expressed in Eq. (15). Here we plot one side of the momentum axis by retaining the term $f_{(-)}$. The reason to do so is that the $f_{(+)}$ term has the same type of momentum distribution on the other side of the momentum axis. The graph is shown in Fig. 2 for $\kappa = 60$, and $\delta x = 1/10$. In this graph we take uniform probability of the photon distribution. This plot shows that the peaks corresponding to the set of joint photon number (n,m) are dependent on the product of ε and ξ [see Eq. (9)]. We analyze η' that contains the dimensionless constants (i.e., ε and ξ) and the joint photon numbers in mode A and B. There is a set of peaks in momentum spectrum for a constant m and over the whole range of n (as we take the example $n = 0 \rightarrow 9$). We note that if the product of these constants is less then a certain number say q then the few peaks (in the momentum distribution spectrum) from the set of adjacent m groups overlap. We show this behavior in Fig. 2(a). In this situation one cannot separate the photon number probability corresponding to these merged peaks. Conversely, if the products of these constants become

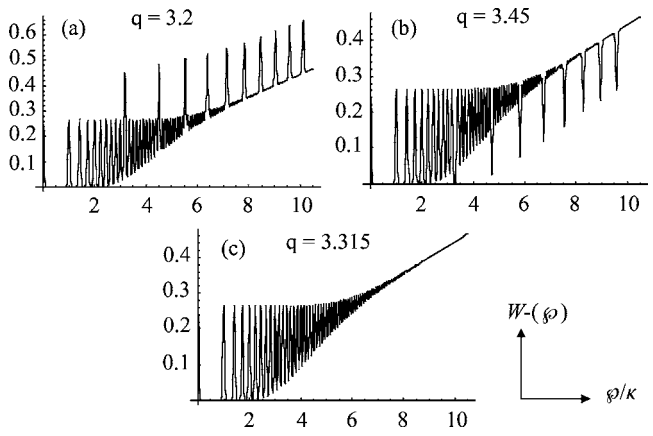

FIG. 2. Momentum distribution spectrum for different values of q. This shows that there is only one value of q at which the number of peaks in the spectrum are equal to the number of set of joint photon numbers in the cavity.

greater than q, then the peaks become very much apart from one another [i.e., Fig. 2(b)]. There is a unique q (under certain conditions that are discussed below) which possesses the characteristics that at this value of q the momentum spectrum peaks have a regular, well-separated structure. We also note that at these specific values of q the momentum patterns become quite similar to the momentum patterns of a single-mode cavity field [Fig. 2(c)]. We realize that at these values of q the recovery of the joint photon statistics is much better.

The selection of q also depends on the summation over the joint field photon number n and m. This selection depends upon the value of the average photon population chosen. As $q = \varepsilon\xi$, ε and ξ are inversely proportional to each other. This shows that at smaller values of coupling ratio (i.e., $\xi = g_A/g_B$), we obtain a larger value of the ratio of wave vectors (i.e., $\varepsilon = k_A/k_B$), that is, at lower values of ξ, the wave vectors are separated apart while at a bigger value of ξ the wave vectors are closer to each other.

We note another point also: If we take the case of single-mode cavity photon statistics [13] and consider a coherent state having an average of three photons then we need to take the summation up to nine over the photon number. The reason for taking the summation up to nine is that the probability of the photons above nine is very small. So, we neglect the contribution of the higher photon number and restrict ourself to up to nine. This gives us data of ten points corresponding to each photon number on the momentum axis. The situation may be compared with the case of two entangled coherent modes, then the summation over the mode A and mode B up to the same number nine gives us the data of 100 points, with each point corresponding to a set of unique joint photon numbers. In conclusion we need to resolve a large number of peaks in momentum distributions spectrum during the measurement of the joint photon statistics of the entangled fields. This requires a very high coupling between the fields and the atom, consequently the q should be a large number. For small average photon numbers, however, we need a relatively small value of q. It should be noted that the number of peaks for the case of entangled field is the square of the number of peaks as compared to a single-mode field-

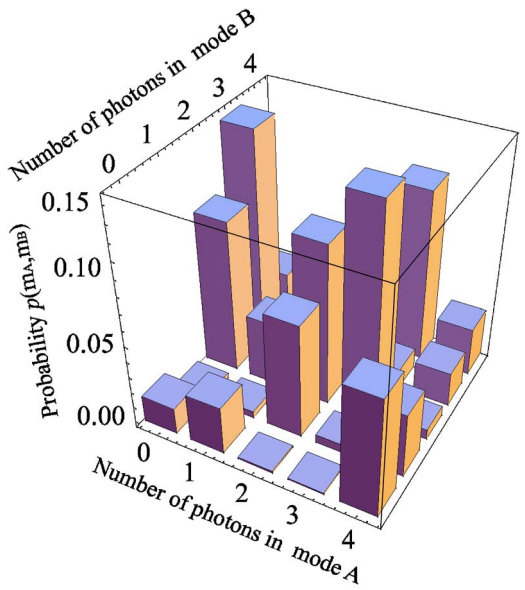

FIG. 3. (Color online) The considered joint photon statistics of the entangled field modes.

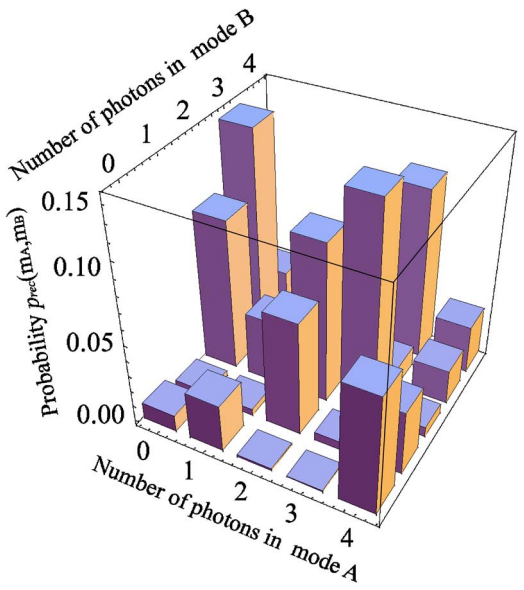

FIG. 5. (Color online) The reconstructed joint photon statistics of the cavity field.

state, so we need a large value of the vacuum Rabi frequency in the case of an entangled field-state to resolve these peaks.

Here is another point, that is, if we define the wave vector of mode A in terms of mode B and the coupling constant of mode B in terms of mode A (which is contrary to the situation we have discussed earlier) then the situation remains the same. In other words the ratio of the ε and ξ remains the same. We have to use the same type of environment in which the coupling of one mode is large than the other.

As an example, we reconstruct the joint photon statistics of the entangled field-state shown in Fig. 3. The number of photons in both modes varies from 0 to 4 as is clear from Fig. 3. We find $q=2.24$ in this particular case. The momentum distribution of the atoms after interacting with the cavity field is shown in Fig. 4. This graph is taken for $\kappa=60$, $\delta x=1/10$, and $q=2.24$. The choice of ε and ξ in q are relative, if one chooses the wave vectors of the two modes close to each other then their should be strong coupling of one mode with respect to the other (i.e., roughly double). This graph also shows that the momentum distribution peaks at the lower photon numbers are well separated and they are nearly merging at higher values of photon numbers. The reason for this behavior is that we need more and more high value of coupling constants to resolve the momentum distribution peaks for higher value. This shows that at higher values of joint photon numbers the error probability will be greater then the lower values of the joint photon numbers. One can resolve this problem by using the high values of the coupling constants. As each peak in the momentum distribution spectrum corresponds to the unique set of joint photon numbers, by knowing the probabilities of the momentum states we can determine the state of the cavity field. We use the same logic to reconstruct the joint photon statistics of the entangled field-state shown in Fig. 5. This graph is taken by using the same set of the values of the different parameters as discussed earlier. The recovery is in good agreement with the original one.

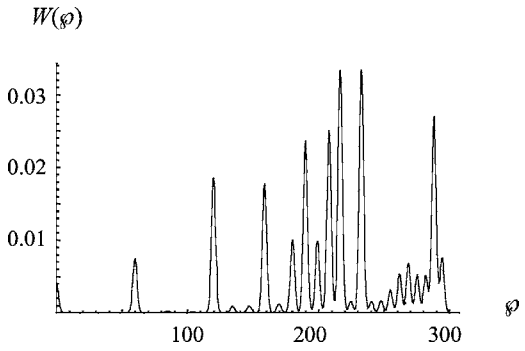

FIG. 4. The momentum distribution spectrum of the atoms when there are two entangled modes in the high-Q cavity. In this graph we chose the parameters $q=2.24$, $\delta x=1/10$, and $\kappa=60$, moreover the summation is taken up to four on both the modes.

Wigner function of two-mode entangled field-state

The joint photon statistics alone cannot give the full information of the entangled field-state. To get the information about the off-diagonal density matrix elements one needs to reconstruct the Wigner function. We start with the definition of the Wigner function described in [26]. In this reference Cahill and Glauber have suggested that the Wigner function of the single mode field [whose photon statistics is $p(m)$] can be reconstructed by displacing the cavity field-state. They have obtained an expression for the Wigner function in terms of displaced photon statistics of the field [26,27].

We realize that the definition of the Wigner function [26] can also be extended for the case of the two-mode field by injecting coherent states α and β. The corresponding displacement operator $D(\alpha)$ and $D(\beta)$ are defined as

$$D(\alpha) = \exp[\alpha a^{\dagger} - \alpha^{*} a], \tag{21}$$

$$D(\beta) = \exp[\beta b^{\dagger} - \beta^{*} b]. \tag{22}$$

The quasiprobability distribution corresponding to the two-mode entangled field-states is defined as

$$\Phi(\alpha, \alpha^{*}, \beta, \beta^{*}) = \frac{1}{\pi^{2}} \mathrm{Tr}[\rho T(\alpha, \beta, s)], \tag{23}$$

where s is the order of products of the field operators. The term $T(\alpha, \beta, s)$ given in [22] is the two-dimensional Fourier transform of the displacement operators $D(\alpha_1)$ and $D(\beta_1)$. We use an alternative expression for $T(\alpha, \beta, s)$, which is useful for our purpose [27],

$$T(\alpha, \beta, s) = \frac{4}{1-s} D(\beta) D(\alpha) \left(\frac{s+1}{s-1} \right)^{a^{\dagger} a + b^{\dagger} b} D^{\dagger}(\alpha) D^{\dagger}(\beta). \tag{24}$$

For $s=0$ one obtains the Wigner distribution. The quasiprobability distribution function defined in Eq. (23) gets the form of the Wigner distribution function for a general state $\rho = |\Psi\rangle\langle\Psi|$,

$$W(\alpha, \alpha^{*}, \beta, \beta^{*}) = \frac{4}{\pi^{2}} \sum_{n,m} (-1)^{n+m} \mathcal{P}(n, m, \alpha, \beta), \tag{25}$$

where $\mathcal{P}(n, m, \alpha, \beta)$ is the displaced photon statistics of the entangled cavity field, i.e.,

$$\mathcal{P}(n, m, \alpha, \beta) = |\langle n, m | D^{\dagger}(\beta) D^{\dagger}(\alpha) | \Psi \rangle|^{2}. \tag{26}$$

Thus the Wigner function of the field can be found directly if the displaced photon statistics $p(n, m, \alpha, \beta)$ is known for all values of α and β.

In the previous section we have given a scheme for the measurement of the joint photon statistics of the undisplaced entangled field-state in two cavities. To get the Wigner function of the entangled state we propose to displace each mode by injecting coherent states $|\alpha\rangle$ and $|\beta\rangle$. Experimentally coupling two resonant classical oscillators to the cavity modes carries out this operation. The joint photon statistics of the displaced entangled field can be obtained by the procedure mentioned earlier, i.e., by the interaction of the three-level atoms with the fields in the Raman-Nath regime. The measuring of the momentum distribution gives the joint photon statistics of the displaced entangled state. By repeating the experiment on an ensemble of identically prepared systems but with different values of α and β, we can reconstruct the Wigner function $W(\alpha, \alpha^{*}, \beta, \beta^{*})$ in a straightforward way as shown in Eq. (25).

IV. CONCLUSION

In this paper, we have discussed a simple scheme for the reconstruction of the joint photon statistics and hence the Wigner function of the *bi*-mode entangled field in a cavity. The probe in this scheme is the momentum states of the atom in the Raman-Nath regime. As a first step towards the measurement of the full quantum state, we propose the reconstruction of the joint photon statistics of the entangled modes. The proposed method can be extended very easily for the measurement of the displaced photon statistics of the cavity fields which leads to the full quantum information in the form of the Wigner function of the *bi*-mode entangled field.

We propose to utilize a V configuration three-level atom in ground state $|b\rangle$. We also suggest to put a slit of width $\delta x \ll \lambda_i$ (i.e., the wave vectors of the electromagnetic modes) so that the atoms are incident on a small portion of the standing wave cavity field. We have seen from our calculations that the momentum probability of the diffracted atoms has a comb of peaks around $x=0$. These peaks show the change in the longitudinal component of the momentum of the atoms and they depend upon the number of interactions (exchange of photon numbers) with the cavity modes. We plot this behavior in Fig. 4 for two entangled modes in the cavity. The critical point in this setup is the selection of the parameters in the equation of the spectrum of the momentum distribution [i.e., Eq. (20)]. The selection should be such that each momentum peak corresponds to a unique set of joint photon number.

We investigate that the momentum peaks corresponding to the different set of joint photon number becomes very much clear and separated from each other if we take the large separation between the coupling constants g_A and g_B. For a given set of g_A and g_B there is a unique value of q . This value of q depends upon the summation over the joint photon number n and m. If we go for a different set of values of g_A and g_B then we have to search for a different value of q. The values of the vacuum Rabi frequencies should be such that the peaks of the momentum distribution corresponding to $m=0$ and $n=0 \rightarrow 9$ (for example) should be separated from the peaks corresponding to the momentum distribution selected to $m=1$ and $n=0 \rightarrow 9$ and so on. In other words, there should be groups of the momentum distribution peaks which have the values n over the whole range and a constant value of m. In the next group of the peaks in the momentum distribution spectrum the values of the n are again over the same whole range but the m is one more then the previous value. Under the conditions discussed above the best recovery of the joint photon statistics of the entangled fields is attained.

As the information of the field photon numbers is present in the momentum distribution, well-separated momentum peaks lead to a nice recovery of the field photon statistics. We get the momentum distribution spectrum of the three-level atoms for $q=2.24$, $\kappa=60$, $\delta x = 1/10$, and summation is taken up to four. Figure 5 illustrates the reconstructed joint photon statistics on the basis of the obtained momentum distribution spectrum. A comparison of original distribution with the reconstructed one displays a good agreement. We also suggest to keep the injection rate of the atoms very low so that there is only one atom interacting with the cavity mode at a time.

ACKNOWLEDGMENTS

The research of M.S.Z. is supported by the Air Force Research Laboratory (Rome, NY), TAMU Telecommunication and Informatics Task Force (TITF) initiative, DARPA

(QuIST), and the Office of Naval Research. A.H.K. would like to thank Manzoor Ikram for helpful discussions on the subject matter.

APPENDIX

The equations of motion for the density matrix elements are obtained:

$$\dot{\rho}^{b,b}_{nm,nm}(x,x',t) = -ig_A k_A\sqrt{n}\{x\rho^{a,b}_{n-1m,nm}(x,x',t) - x'\rho^{b,a}_{nm,n-1m}(x,x',t)\} - ig_B k_B\sqrt{m}\{x\rho^{c,b}_{nm-1,nm}(x,x',t) - x'\rho^{b,c}_{nm,nm-1}(x,x',t)\}, \quad \text{(A1a)}$$

$$\dot{\rho}^{a,a}_{n-1m,n-1m}(x,x',t) = -ig_A k_A\sqrt{n}\{x\rho^{b,a}_{nm,n-1m}(x,x',t) - x'\rho^{a,b}_{n-1m,nm}(x,x',t)\}, \quad \text{(A1b)}$$

$$\dot{\rho}^{c,c}_{nm-1,nm-1}(x,x',t) = -ig_B k_B\sqrt{m}\{x\rho^{b,c}_{nm,nm-1}(x,x',t) - x'\rho^{c,b}_{nm-1,nm}(x,x',t)\}, \quad \text{(A1c)}$$

$$\dot{\rho}^{b,a}_{nm,n-1m}(x,x',t) = -ig_A k_A\sqrt{n}\{x\rho^{a,a}_{n-1m,n-1m}(x,x',t) - x'\rho^{b,b}_{nm,nm}(x,x',t)\} - ig_B k_B\sqrt{m}x\rho^{c,a}_{nm-1,n-1m}(x,x',t), \quad \text{(A1d)}$$

$$\dot{\rho}^{b,c}_{nm,nm-1}(x,x',t) = -ig_B k_B\sqrt{m}\{x\rho^{c,c}_{nm-1,nm-1}(x,x',t) - x'\rho^{b,b}_{nm,nm}(x,x',t)\} - ig_A k_A\sqrt{n}x\rho^{a,c}_{n-1m,nm-1}(x,x',t), \quad \text{(A1e)}$$

$$\dot{\rho}^{a,b}_{n-1m,nm}(x,x',t) = -ig_A k_A\sqrt{n}\{x\rho^{b,b}_{nm,nm}(x,x',t) - x'\rho^{a,a}_{n-1m,n-1m}(x,x',t)\} + ig_B k_B\sqrt{m}x'\rho^{a,c}_{n-1m,nm-1}(x,x',t), \quad \text{(A1f)}$$

$$\dot{\rho}^{c,b}_{nm-1,nm}(x,x',t) = -ig_B k_B\sqrt{m}\{x\rho^{b,b}_{nm,nm}(x,x',t) - x'\rho^{c,c}_{nm-1,nm-1}(x,x',t)\} + ig_A k_A\sqrt{n}x'\rho^{c,a}_{nm-1,n-1m}(x,x',t), \quad \text{(A1g)}$$

$$\dot{\rho}^{a,c}_{n-1m,nm-1}(x,x',t) = -ig_A k_A\sqrt{n}x\rho^{b,c}_{nm,nm-1}(x,x',t) + ig_B k_B\sqrt{m}x'\rho^{a,b}_{n-1m,nm}(x,x',t), \quad \text{(A1h)}$$

$$\dot{\rho}^{c,a}_{nm-1,n-1m}(x,x',t) = -ig_B k_B\sqrt{m}x\rho^{b,a}_{nm,n-1m}(x,x',t) + ig_A k_A\sqrt{n}x'\rho^{c,b}_{nm-1,n1m}(x,x',t), \quad \text{(A1i)}$$

where we use the notation for the density matrix elements as

$$\rho^{b,b}_{nm,nm}(x,x',t) = \langle x',n,m,b|\rho|b,n,m,x\rangle,$$

$$\rho^{a,a}_{n-1m,n-1m}(x,x',t) = \langle x',n-1,m,a|\rho|a,n-1,m,x\rangle,$$

$$\rho^{c,c}_{nm-1,nm-1}(x,x',t) = \langle x',n,m-1,c|\rho|c,n,m-1,x\rangle,$$

$$\rho^{b,a}_{nm,n-1m}(x,x',t) = \langle x',n,m,b|\rho|a,n-1,m,x\rangle,$$

$$\rho^{b,c}_{nm,nm-1}(x,x',t) = \langle x',n,m,b|\rho|c,n,m-1,x\rangle,$$

$$\rho^{a,b}_{n-1m,nm}(x,x',t) = \langle x',n-1,m,a|\rho|b,n,m,x\rangle,$$

$$\rho^{c,b}_{nm-1,nm}(x,x',t) = \langle x',n,m-1,c|\rho|b,n,m,x\rangle,$$

$$\rho^{a,c}_{n-1m,nm-1}(x,x',t) = \langle x',n-1,m,a|\rho|c,n,m-1,x\rangle,$$

$$\rho^{c,a}_{nm-1,n-1m}(x,x',t) = \langle x',n,m-1,c|\rho|a,n-1,m,x\rangle.$$

The Laplace transform of Eqs. (A1a)–(A1i) is given by the following set of equations:

$$s\pounds(\rho)^{b,b}_{nm,nm}(x,x',t) + i\alpha x\pounds(\rho)^{a,b}_{n-1m,nm}(x,x',t) - i\alpha x'\pounds(\rho)^{b,a}_{nm,n-1m}(x,x',t) + i\beta x\pounds(\rho)^{c,b}_{nm-1,nm}(x,x',t) - i\beta x'\pounds(\rho)^{b,c}_{nm,nm-1}(x,x',t) = \rho^{b,b}_{nm,nm}(x,x',0), \quad \text{(A2a)}$$

$$s\pounds(\rho)^{a,a}_{n-1m,n-1m}(x,x',t) + i\alpha x\pounds(\rho)^{b,a}_{nm,n-1m}(x,x',t) - i\alpha x'\pounds(\rho)^{a,b}_{n-1m,nm}(x,x',t) = 0, \quad \text{(A2b)}$$

$$s\pounds(\rho)^{c,c}_{nm-1,nm-1}(x,x',t) + i\beta x\pounds(\rho)^{b,c}_{nm,nm-1}(x,x',t) - i\beta x'\pounds(\rho)^{c,b}_{nm-1,nm}(x,x',t) = 0, \quad \text{(A2c)}$$

$$s\pounds(\rho)^{b,a}_{nm,n-1m}(x,x',t) + i\alpha x\pounds(\rho)^{a,a}_{n-1m,n-1m}(x,x',t) - i\alpha x'\pounds(\rho)^{b,b}_{nm,nm}(x,x',t) + i\beta x\pounds(\rho)^{c,a}_{nm-1,n-1m}(x,x',t) = 0, \quad \text{(A2d)}$$

$$s\pounds(\rho)^{b,c}_{nm,nm-1}(x,x',t) + i\beta x\pounds(\rho)^{c,c}_{nm-1,nm-1}(x,x',t) - i\beta x'\pounds(\rho)^{b,b}_{nm,nm}(x,x',t) + i\alpha x\pounds(\rho)^{a,c}_{n-1m,nm-1}(x,x',t) = 0, \quad \text{(A2e)}$$

$$s\pounds(\rho)^{a,b}_{n-1m,nm}(x,x',t) + i\alpha x\pounds(\rho)^{b,b}_{nm,nm}(x,x',t) - i\alpha x'\pounds(\rho)^{a,a}_{n-1m,n-1m}(x,x',t) - i\beta x'\pounds(\rho)^{a,c}_{n-1m,nm-1}(x,x',t) = 0, \quad \text{(A2f)}$$

$$s\pounds(\rho)^{c,b}_{nm-1,nm}(x,x',t) + i\beta x\pounds(\rho)^{b,b}_{nm,nm}(x,x',t) - i\beta x'\pounds(\rho)^{c,c}_{nm-1,nm-1}(x,x',t) - i\alpha x'\pounds(\rho)^{c,a}_{nm-1,n-1m}(x,x',t) = 0, \quad \text{(A2g)}$$

$$s\pounds(\rho)^{a,c}_{n-1m,nm-1}(x,x',t) + i\alpha x\pounds(\rho)^{b,c}_{nm,nm-1}(x,x',t) - i\beta x'\pounds(\rho)^{a,b}_{n-1m,nm}(x,x',t) = 0, \quad \text{(A2h)}$$

$$s\pounds(\rho)^{c,a}_{nm-1,n-1m}(x,x',t) + i\beta x\pounds(\rho)^{b,a}_{nm,n-1m}(x,x',t) - i\alpha x'\pounds(\rho)^{c,b}_{nm-1,n1m}(x,x',t) = 0, \quad \text{(A2i)}$$

where in the above set of equations $\alpha = g_A k_A \sqrt{n}$ and $\beta = g_B k_B \sqrt{m}$. We also make use of the initial condition that at $t=0$, the atoms are in ground state, i.e.,

$$\rho^{b,b}_{nm,nm}(x,x',0) = \rho^{b,b}_{nm,nm}(x,x',0) \quad \text{(A3)}$$

and

$$\begin{aligned}\rho^{a,a}_{n-1m,n-1m}(x,x',0) &= \rho^{c,c}_{nm-1,nm-1}(x,x',0) = \rho^{b,a}_{nm,n-1m}(x,x',0) \\ &= \rho^{b,c}_{nm,nm-1}(x,x',0) = \rho^{a,b}_{n-1m,nm}(x,x',0) \\ &= \rho^{a,c}_{n-1m,nm-1}(x,x',0) = \rho^{c,a}_{nm-1,n-1m}(x,x',0) \\ &= \rho^{c,b}_{nm-1,nm}(x,x',0) = 0. \quad \text{(A4)}\end{aligned}$$

Now we solve the set of linear coupled differential equations [i.e., (A2a)–(A2i)] and get the solution in terms of the Laplacians of the density matrix elements

$$\pounds(\rho)^{a,a}_{n-1m,n-1m}(x,x',t) = \frac{2\alpha^2 sxx'}{s^4 + (\alpha^2+\beta^2)^2(x^2-x'^2)^2 + 2(\alpha^2+\beta^2)s^2(x^2+x'^2)} \times \rho^{b,b}_{nm,nm}(x,x',0), \quad \text{(A5a)}$$

$$\pounds(\rho)^{b,b}_{nm,nm}(x,x',t) = \frac{s[s^2 + (\alpha^2+\beta^2)(x^2+x'^2)]}{s^4 + (\alpha^2+\beta^2)^2(x^2-x'^2)^2 + 2(\alpha^2+\beta^2)s^2(x^2+x'^2)} \times \rho^{b,b}_{nm,nm}(x,x',0), \quad \text{(A5b)}$$

$$\pounds(\rho)^{c,c}_{nm-1,nm-1}(x,x',t) = \frac{2\beta^2 sxx'}{s^4 + (\alpha^2+\beta^2)^2(x^2-x'^2)^2 + 2(\alpha^2+\beta^2)s^2(x^2+x'^2)} \times \rho^{b,b}_{nm,nm}(x,x',0), \quad \text{(A5c)}$$

$$\pounds(\rho)^{a,b}_{n-1m,nm}(x,x',t) = \frac{-i\alpha x[s^2 + (\alpha^2+\beta^2)(x^2-x'^2)]}{s^4 + (\alpha^2+\beta^2)^2(x^2-x'^2)^2 + 2(\alpha^2+\beta^2)s^2(x^2+x'^2)} \times \rho^{b,b}_{nm,nm}(x,x',0), \quad \text{(A5d)}$$

$$\pounds(\rho)^{b,a}_{nm,n-1m}(x,x',t) = \frac{i\alpha x'[s^2 - (\alpha^2+\beta^2)(x^2-x'^2)]}{s^4 + (\alpha^2+\beta^2)^2(x^2-x'^2)^2 + 2(\alpha^2+\beta^2)s^2(x^2+x'^2)} \times \rho^{b,b}_{nm,nm}(x,x',0), \quad \text{(A5e)}$$

$$\pounds(\rho)^{a,c}_{n-1m,nm-1}(x,x',t) = \frac{2\alpha\beta sxx'}{s^4 + (\alpha^2+\beta^2)^2(x^2-x'^2)^2 + 2(\alpha^2+\beta^2)s^2(x^2+x'^2)} \times \rho^{b,b}_{nm,nm}(x,x',0), \quad \text{(A5f)}$$

$$\pounds(\rho)^{c,a}_{nm-1,n-1m}(x,x',t) = \frac{2\alpha\beta sxx'}{s^4 + (\alpha^2+\beta^2)^2(x^2-x'^2)^2 + 2(\alpha^2+\beta^2)s^2(x^2+x'^2)} \times \rho^{b,b}_{nm,nm}(x,x',0), \quad \text{(A5g)}$$

$$\pounds(\rho)^{b,c}_{nm,nm-1}(x,x',t) = \frac{-i\beta x'[s^2 - (\alpha^2+\beta^2)(x^2-x'^2)]}{s^4 + (\alpha^2+\beta^2)^2(x^2-x'^2)^2 + 2(\alpha^2+\beta^2)s^2(x^2+x'^2)} \times \rho^{b,b}_{nm,nm}(x,x',0), \quad \text{(A5h)}$$

$$\pounds(\rho)^{c,b}_{nm-1,nm}(x,x',t) = \frac{-i\beta x[s^2 + (\alpha^2+\beta^2)(x^2-x'^2)]}{s^4 + (\alpha^2+\beta^2)^2(x^2-x'^2)^2 + 2(\alpha^2+\beta^2)s^2(x^2+x'^2)} \times \rho^{b,b}_{nm,nm}(x,x',0), \quad \text{(A5i)}$$

Now the set of equations (A5a)–(A5i) are no longer coupled, so, we solve only the equations of interest. These are the equations of the populations of the atoms in either of their internal states. The inverse Laplace transform of this set of equations gives the equations of motion for the density matrix elements of the atomic states expressed in Eqs. (5)–(7).

[1] P. W. Shor, SIAM J. Comput. **26**, 1484 (1997); L. K. Grover, Phys. Rev. Lett. **79**, 325 (1997); **79**, 4709 (1997).

[2] C. H. Bennett, G. Brassard, C. Crepeau, R. Jozsa, A. Peres, and W. K. Wootters, Phys. Rev. Lett. **70**, 1895 (1993).

[3] C. H. Bennett and S. J. Wiesner, Phys. Rev. Lett. **69**, 2881 (1992).

[4] S. F. Huelga, C. Macchiavello, T. Pellizzari, A. K. Ekert, M. B. Plenio, and J. I. Cirac, Phys. Rev. Lett. **79**, 3865 (1997); S. Bose, V. Vedral, and P. L. Knight, Phys. Rev. A **57**, 822 (1998); M. Murao, M. B. Plenio, S. Popescu, V. Vedral, and P. L. Knight, *ibid.* **57**, R4075 (1998); A. Karlsson, M. Koashi, and N. Imoto, *ibid.* **59**, 162 (1999); P. W. Shor, Phys. Rev. A **52**, R2493 (1995).

[5] D. T. Smithey, M. Beck, M. G. Raymer, and A. Faridani, Phys. Rev. Lett. **70**, 1244 (1993); S. Schiller, G. Breitenbach, S. F. Pereira, T. Muller, and J. Mlynek, *ibid.* **77**, 2933 (1996).

[6] K. Vogel and H. Risken, Phys. Rev. A **40**, R2847 (1989).

[7] M. Brune, S. Haroche, V. Lefevre, J. M. Raimond, and N. Zagury, Phys. Rev. Lett. **65**, 976 (1990); M. Brune, S. Haroche, J. M. Raimond, L. Davidovich, and N. Zagury, Phys. Rev. A **45**, 5193 (1992).

[8] M. S. Zubairy, Phys. Lett. A **222**, 91 (1996); P. J. Bardroff, E.

Mayr, and W. P. Schleich, Phys. Rev. A **51**, 4963 (1995); M. S. Zubairy, *ibid.* **57**, 2066 (1998); T. Azim and M. S. Zubairy, Phys. Lett. A **250**, 344 (1996); M. Mahmoudi, H. Tajalli, and M. S. Zubairy, J. Opt. B: Quantum Semiclassical Opt. **2**, 315 (2000).

[9] M. J. Holland, D. F. Walls, and P. Zoller, Phys. Rev. Lett. **67**, 1716 (1991); A. M. Herkommer, V. M. Akulin, and W. P. Schleich, *ibid.* **69**, 3298 (1992).

[10] M. Freyberger and A. M. Herkommer, Phys. Rev. Lett. **72**, 1952 (1994).

[11] P. J. Bardroff, E. Mayr, and W. P. Schleich, Phys. Rev. A **51**, 4963 (1995); P. J. Bardroff, E. Mayr, W. P. Schleich, P. Domokos, M. Brune, J. M. Raimond, and S. Haroche, *ibid.* **53**, 2736 (1996).

[12] A. A. Khan and M. S. Zubairy, Phys. Lett. A **254**, 301 (1997).

[13] Ashfaq H. Khosa and M. S. Zubairy (unpublished).

[14] Ashfaq H. Khosa, M. Ikram, and M. S. Zubairy, Phys. Rev. A **70**, 052312 (2004).

[15] A. F. Bernhardt and B. W. Shore, Phys. Rev. A **23**, 1290 (1981); R. J. Cook and A. F. Bernhardt, *ibid.* **18**, 2533 (1978).

[16] M. Marte and S. Stenholm, Appl. Phys. B: Photophys. Laser Chem. **B54**, 443 (1992).

[17] B. C. Sanders, Phys. Rev. A **45**, 6811 (1992); N. A. Ansari and V. I. Man'ko, *ibid.* **50**, 1942 (1994); S. M. Tan, D. F. Walls, and M. J. Collett, Phys. Rev. Lett. **66**, 252 (1991); M. O. Scully, B. G. Englert, and H. Walther, Nature (London) **351**, 111 (1991).

[18] M. G. Raymer, D. F. McAlister, and U. Leonhardt, Phys. Rev. A **54**, 2397 (1996).

[19] M. S. Kim and G. S. Agarwal, Phys. Rev. A **59**, 3044 (1999).

[20] M. S. Kim, G. Antesberger, C. T. Bodendorf, and H. Walther, Phys. Rev. A **58**, R65 (1998); M. Wilkens and P. Meystre, *ibid.* **43**, 3832 (1991); S. M. Dutra, P. L. Knight, and H. Moya-Cessa, *ibid.* **48**, 3168 (1993).

[21] H. Kuhn, D.-G. Welsch, and W. Vogel, Phys. Rev. A **51**, 4240 (1995).

[22] M. Ikram and M. S. Zubairy, Phys. Rev. A **65**, 044305 (2002).

[23] M. França Santos, L. G. Lutterbach, and L. Davidovich, J. Opt. B: Quantum Semiclassical Opt. **3**, 15214 (2001).

[24] M. Vasilyev, S. K. Choi, P. Kumar, and G. MauroDAriano, Phys. Rev. Lett. **84**, 2354 (2000).

[25] K. Banaszek and K. Wodkiewicz, Phys. Rev. Lett. **76**, 4344 (1996).

[26] K. E. Cahill and R. J. Glauber, Phys. Rev. **177** , 1857 (1969); **177**, 1882 (1969).

[27] L. G. Lutterbach and L. Davidovich, Phys. Rev. Lett. **78**, 2547 (1997).